Article:
Kechnit, D., Tshimanga, R.M., Ammari, A. et al. (5 more authors) (2024) Bathymetry and discharge estimation in large and data-scarce rivers using an entropy-based approach. Hydrological Sciences Journal, 69 (15). pp. 2109-2123. ISSN: 0262-6667

https://doi.org/10.1080/02626667.2024.2402933

Bathymetry and Discharge Estimation in Large and Data-Scarce Rivers Using an Entropy-Based Approach

Djamel Kechnit [a]*, Raphael M. Tshimanga [a], Abdelhadi Ammari [b], Mark A. Trigg [c], Andrew B. Carr [c], Farhad Bahmanpouri [d], Silvia Barbetta [d] and Tommaso Moramarco [d]

[a] *Congo Basin Water Resources Research Center (CRREBaC) & Regional School of Water (ERE), University of Kinshasa (UNIKIN), DRC.*

[b] *National Higher School of Hydraulics (ENSH), Algeria.*

[c] *School of Civil Engineering, University of Leeds, UK.*

[d] *Research Institute for Geo-Hydrological Protection - National Research Council (CNR IRPI), Perugia, Italy.*

*Corresponding author. E-mail: d.kechnit@ensh.dz

Abstract

This study implements an entropy theory-based approach to infer bathymetry for 29 selected cross-sections along a 1740 km reach of the Congo River. A Genetic Algorithm optimisation approach is used based on near-surface velocity measurements analysis to generate a random sample of 1000 bathymetry profiles from which the analysis is carried out. The resulting simulated bathymetry shows good agreement compared to the measurements obtained via ADCP, with a correlation that varies from 0.49 to 0.88. The bathymetry results are subsequently used to estimate the 2D cross-sectional flow velocity distribution and, consequently, to calculate the river discharge. The mean errors observed for flow area, discharge, and mean velocity are found to be equal to 2.7%, 1.3%, and 1%, respectively. This study demonstrates, for the first time, the successful application of an entropy-based approach to estimate bathymetry and discharge in large rivers and provide significant implications for remote sensing applications.

Keywords: bathymetry, discharge, entropy approach, large rivers, near-surface velocity.

1 Introduction

Africa hosts some of the world's largest rivers, playing a crucial part in maintaining vast ecosystems on the continent and supporting the livelihoods of millions of people. The Nile River is the longest in the world (Gebrehiwot et al., 2019), and the Congo River Basin (CRB), is the second largest in the world after the Amazon in terms of drainage area and discharge. Other major rivers such as the Niger, Zambezi, and Limpopo, are equally essential for the ecological functions and human populations within their respective basins (Mitchell, 2013; Gaye and Tindimugaya, 2019).

Extensive research has been conducted to shed light on the challenges associated with sustainable water management in the African river basins. Despite these efforts, our current understanding of the dynamics of water resources in the continent remains inadequate. This limited knowledge poses a significant obstacle to the implementation of effective water resources management strategies across various spatial and temporal scales. According to Tshimanga (2022), the lack of information on water resources in African River basins is a critical impediment to their sustainable management and development. This is primarily attributed to the paucity of hydro-meteorological monitoring networks, limited financial resources and expertise for water resources monitoring, and insufficient field investigations. Consequently, developing new methods for monitoring large rivers in Africa such as the Congo River is of paramount importance for supporting a global agenda focused on climate change adaptation and achieving sustainable development goals. Recent studies show that the CRB provides multiple goods and services in terms of water resources (Runge, 2022). However, implementing appropriate river basin management strategies within the CRB is particularly challenging due to the complex nature of hydrodynamic processes associated with the lack of field data (Trigg and Tshimanga, 2020; Alsdorf et al., 2016). Currently, there are several initiatives under discussion for the CRB. Some of these initiatives include inter-basin

water transfer, optimisation of the regional river navigation corridor to connect the riparian countries, development of the African hydropower grid from the Grand Inga Dam, and maintenance of the recently discovered vast complex of peat lands of the Cuvette Central. All these initiatives require supporting water resources information, which is currently critically lacking or will be difficult to obtain in the decade through direct field measurements. For instance, accurate river discharge, water level, sediment transport, and bathymetry are essential for improving water resources management.

Bathymetry is an important parameter for large river management, especially in the CRB as it provides information on the river topography and the flow conveyance capacity of the river system. The lack of bathymetric information at the required management scale in the CRB poses challenges for developing effective models to enhance water resources management. Several recent studies have attempted to estimate variables of the Congo River that relate to bathymetry. Some of these studies include:

- Learning regression method (ELQ) to estimate river discharges based on remotely sensed measurements of water levels, effective river widths, and multi-temporal surface water extent (Kim et al., 2019);
- Assessment of spatial variability in the water surface slope of the main stem of the Congo River through *in-situ* data to identify implications for hydrodynamic studies of large rivers compared to satellite altimetry (Carr et al., 2019);
- Enhancement of the global estimation of river bathymetry and discharge using surface water and ocean topography (SWOT), based on the integration of hydrodynamic modelling and field measurements (Jung et al., 2010; Revel et al., 2018; Trigg et al., 2021);
- Estimation of bathymetry in low gradient multi-thread channel systems using Manning's equation in-channel flow conditions (Carr et al., 2022);

- New measurements of water dynamics and sediment transport along the middle reach of the Congo River and the Kasai tributary (Tshimanga et al., 2022a).

However, most of these studies using remote sensing data have encountered challenges due to high turbidity and suspended sediment load, which limit the penetration depth of remote sensing signal, even though the Congo River has a relatively low sediment load compared to other large rivers. Furthermore, the constantly changing river morphology, including the presence of sandbars and islands, makes it difficult to accurately model and estimate the riverbed topography.

Moramarco et al. (2019) developed an efficient approach for estimating bathymetry based on entropy theory, which relies on the analysis of near-surface velocity. Surface flow velocity can be measured using ground-based technologies such as Acoustic Doppler Current Profiler (ADCP), airborne remote sensing instruments (Masafu et al., 2022), or earth observation satellites (Legleiter and Kinzel, 2021; Schumann and Everard, 2022). Entropy theory has been widely used by researchers to assess discharge, velocity distributions, and other variables related to river morphology (Chiu, 1987, 1988, 1989; Moramarco et al., 2004, 2010, 2011, 2013, 2017; Termini and Moramarco, 2016; Ammari et al., 2017, 2022; Bahmanpouri et al., 2022a; Singh and Khosa, 2023). Recently, Patel and Sarkar (2023) developed an indirect flow measurement technique to estimate discharge at ungauged stations on the Brahmani River and demonstrated its accuracy compared to a numerical model. The entropy approach has also shown promise for analysing 2D velocity distributions in large rivers. Bahmanpouri et al. (2022b) applied the entropy theory in the confluence zone of the Rio Negro and Rio Solimões, one of the largest confluences of the Amazon River, and found that the error observed was less than 15% compared to ADCP measurements.

One of the key advantages of this method is its ability to provide accurate estimates with minimal fieldwork, as it only requires sampling a few surface velocities across the river. This makes it particularly appealing for remote sensing applications where airborne or satellite-based surface velocity retrieval methods can be leveraged. Recent studies have demonstrated the effectiveness of using aerial and satellite imagery to estimate river flow velocities, with Legleiter et al. (2023) developing a moving aircraft river velocimetry (MARV) framework that uses aerial imagery to accurately estimate flow velocities in large, turbid rivers. Furthermore, ongoing research into satellite-based surface velocity retrieval has shown promising results, with Everard et al. (2023), Masafu et al. (2023), and Masafu and Williams (2024) demonstrating the ability to accurately measure surface flow speed in medium and large rivers using high-resolution satellite video. The development of these satellite-based methods holds significant potential for applying the entropy-based approach in ungauged and large river systems.

The current entropy-based approach, as applied in previous research, has shown promise in discharge monitoring. However, certain limitations are noted, particularly those related to bathymetry. In most previous studies, bathymetry data are considered an observed quantity and used to infer a 2D velocity distribution and discharge, or they are estimated only in small and medium rivers with widths ranging from 50 to 500 meters. The entropy approach has not previously been applied to large rivers, as this approach is challenging to implement where the bathymetry is difficult to measure, or sometimes completely unknown. Therefore, the main objective of this research is to assess the effectiveness of the entropy approach in estimating bathymetry for very large rivers. Subsequently, the derived bathymetry is used to estimate 2D velocity distributions and discharge, which are compared to observations, thus allowing for a thorough error analysis. Additionally, a new aspect of this research here is to apply the approach to the

very complex multi-channel morphology of the Congo River, where the bathymetry is highly irregular and poses difficulties even for *in-situ* measurements.

2 The entropy approach: theoretical background

The flow velocity distribution in a cross-section based on the entropy approach was first proposed by Chiu (1989) and then simplified by Moramarco et al. (2004). This approach allows estimation of the entropy-based velocity profile along the verticals as:

$$u(x,y) = \frac{u_{max(x)}}{M}\ ln\left[1 + (e^M - 1)\ \frac{y}{D(x)-h(x)}\ \exp(1 - \frac{y}{D(x)-h(x)})\ \right] \quad (1)$$

where u is the time-averaged velocity; $u_{max(x)}$ is the maximum value of u at a distance x from the left bank; y is the distance of the velocity point from the river bottom; $D(x)$ is the flow depth; $h(x)$ is the dip, i.e., the depth of $u_{max}(x)$ below the water surface when the maximum velocity occurs at the water surface, $h(x) = 0$; M is the entropic parameter, characteristic of the cross-section that can be estimated based on pairs of measured mean and maximum river flow velocity, (u_m, u_{MAX}) respectively, using the linear entropic relation (Chiu, 1989):

$$\frac{u_m}{u_{MAX}} = \frac{e^M}{e^M - 1} - \frac{1}{M} = \Phi(M) \quad (2)$$

$\Phi(M)$ is found to be constant for many measurements in the same cross-section even when taking into consideration the high and low flow conditions (Ammari and Remini, 2010).

The estimation of the 2D velocity distribution in a river cross-section can be developed using Eq. (1). However, the quantities that describe the bathymetry of the cross-section are required, i.e., the water depth D. Such information is rarely available. In this context,

Moramarco et al., (2013; 2019) developed an approach for the estimation of the bathymetry, which exploits the principle of maximum entropy inferring the Eq. (3):

$$D(x) = \frac{D_{MAX}}{W}\, ln\left[1 + (e^{W} - 1)\, \frac{u_{max}\,(x)}{u_{MAX}}\right] \quad (3)$$

where $D(x)$ represents the mean flow depth at distance x from the left bank; D_{MAX} is the maximum flow depth in the cross-section; $u_{max}\,(x)$ is the maximum velocity; u_{MAX} is the maximum velocity in the cross-section u_{MAX} = max ($u_{max}(x)$) = max $(U_{surface}(x))$; W is the entropy parameter that depends on the ratio between the mean, D_m, and the maximum, D_{MAX}, flow depth in the cross-section:

$$\frac{D_m}{D_{MAX}} = \frac{e^{W}}{e^{W}-1} - \frac{1}{W} = \emptyset(W) \quad (4)$$

$\emptyset\,(W)$ represents the ratio between the pairs (D_m, D_{MAX}), a function of W. The application of Eq. (3) is related to the determination of the entropy parameter W and the availability of measurements of the pairs (D_m, D_{MAX}).

3 Study Area

The CRB is recognised as one of the largest and most ecologically diversified river systems in the world, with a mean annual discharge of 41,000 m^3/s and a catchment area of 3.7 $x10^6$ km^2 (Tshimanga et al., 2022b). The CRB comprises nine countries including, Angola, Burundi, Cameroon, Central African Republic, Republic of Congo, Democratic Republic of Congo, Rwanda, Tanzania, and Zambia (Trigg et al., 2022a). This region is of great ecological significance due to its vast forest cover, diverse wildlife, and the crucial role that it plays in regulating the global climate.

According to Tshimanga et al. (2022b), three major reaches are identified along the main course of the Congo River. There is the upper reach that starts on the Katanga Plateaus, running north until the Boyoma Falls at Kisangani, known as Lualaba, thus

draining a basin area of about 960,000 km^2. This is followed by the middle reach that encompasses the region between the cities of Kisangani and Kinshasa, where the river forms an arc that crosses the equator twice as it runs through the vast swampy basin of the Cuvette Central, a shallow depression along the equatorial line. Along this reach, the river drops only 115 m over 1700 km. In the Cuvette Centrale, the river depths are shallow and vary from 5 to 10 m, and the morphology of the river takes a very complex multi-channel form with a width ranging up to 10 km. The middle reach differs greatly from the upper and the lower reaches, with a surface slope averaging around 5.5 cm/km (O'Loughlin et al., 2020). The middle reach runs towards the city of Kinshasa, and at this location, the total basin area is about 3.6 $x10^6$ km^2. Finally, the lower reach extends to the outlet of the Congo River, the Atlantic Ocean, reaching a total basin drainage area of about 3.7 $x10^6$ km^2.

Major hydrographic features of vast lakes, floodplains, wetlands, peatlands and islands characterise the Congo River's main course from its source to the mouth. At the outlet of the Cuvette Central, the river course enters a stretch known as the Chenal, 220 km long, from Tchumbiri to Kinshasa. In this section, the channel is confined between low hills and follows a single narrow channel, with a 900 -1,600 m width, and depths up to 40 m. A circular riverine water body, the Pool Malebo, marks the end of the Chenal before the Congo River enters its lower part downstream of Kinshasa (Kechnit et al., 2024). The lower reach extends from the Pool Malebo to the Atlantic Ocean (see Fig. (1))

The CRB is an area with significant potential for the development of water resources. It offers a wide range of benefits and services, including generation of hydroelectric power, provision of water, support for fisheries, and opportunities for large-scale irrigated agriculture. In terms of navigation, the extensive river network spans approximately 25000 km (including lake routes) and enables inland navigation,

promoting connectivity among the riparian nations (Tshimanga et al., 2022c). Trigg et al. (2022b) state that there are 17867 km of navigable channels, excluding lakes. These channels are divided into three categories based on the draft of ships that can safely navigate them, taking into account the normal water depth that allows for navigability in both low and high flow seasons: Category 1 (1.30m – 2.0m), Category 2 (1m – 1.30m), and Category 3 (0.5m – 1m) (CICOS, 2023). The middle reach of the Congo River mainstream is classified as Category 1 (see Supplementary material, Figure S1), which represents the deepest reach in the Congo River.

4 Material and Methods

4.1 Data Acquisition

Several field investigations using Acoustic Doppler Current Profiler (ADCP) have been carried out in the CRB (Trigg et al., 2021; Trigg et al., 2022a; Tshimanga et al., 2022a; Carr et al., 2022) to collect data on discharge and bathymetry. Alsdorf et al. (2016) state that the limited availability of *in-situ* data and investigation has been a major obstacle to scientific research in the CRB. The ADCP measurements used in this study were collected from several fieldwork campaigns (Tshimanga et al., 2022a). The first set of measurements carried out between Kunzulu and Kisangani (about 1500 km), was conducted as part of the Congo River Users Hydraulics and Morphology (CRuHM) project, and the Congo Basin Water Resources Research Center (CRREBaC). This project is a research and capacity-building initiative funded by the Royal Society of the United Kingdom (Bate et al., 2024). The second set of measurements, conducted by the Congo Basin Water Resources Research Center (https://www.crrebac.org) and the Congo River authority in the Democratic Republic of Congo (RVF), covered the transect from

Maluku to the outlet of the Pool Malebo. The survey was conducted between 2021 and 2022.

Fig. 2 illustrates the middle reach of the Congo River, which spans from Kisangani to Kinshasa, covering a distance of 1740 km. The surveys primarily focused on the main reach of the river, where an ADCP was deployed. Additionally, some tributaries were also included in the investigation. The TRDI River Ray ADCP with 600 kHz with a maximum depth range of 60 m and a blanking zone estimated at 16 cm was used for field measurements. The deployment method involved mounting the ADCP on a "mobile boat" while continuously recording the measurements. The selection of the measurement transect in the middle reach was based on careful consideration of the water course's geomorphology, including the presence of the Chenal, multi-thread channel, and the Pool Malebo. The feasibility of conducting measurements was also taken into account, especially in challenging areas such as the middle reach with multi-thread channels.

This research aims to exploit two primary components: (i) flow surface velocity, which will be used as input data for the entropy theory, and (ii) measured bathymetry data, which will serve as validation data for the simulated bathymetry results.

4.2 Methodology

The estimation of bathymetry is mainly based on the application of Eq. (3). To this end, all the included variables in this expression must be identified. The approach is suggested by Moramarco et al. (2019) and adopted for large rivers. The process of estimating the different variables and applying Eq. (3) can be summarised as follows:

4.2.1 Determination (u_{surf}, u_{MAX}):

Assuming that the maximum velocity at the surface, the maximum velocity in each vertical along the x-axis will be equal to the surface velocity, (u_{surf}), i.e.:

- $u_{max}(x) = u_{surf}(x)$.
- u_{MAX} =max (u_{max} (x)) = max (u_{surf} (x)).

u_{surf} can be derived using ADCP by selecting the value from the first bin above the surface blanking zone for each vertical along the width of the cross-section.

4.2.2 Determination of the entropy parameter W:

The determination of W is carried out by Eq. (4), which primarily relies on the pairs (D_m, D_{MAX}). The estimation of W can be evaluated in two different scenarios:

- Scenario (a): W is a calibration parameter that is missing and it will be estimated as described in section 4.2.4.
- Scenario (b): The Congo River can be divided into different main reaches based on the different morphology of the watercourse (i.e., Pool Malebo, Chenal, and multi-thread). Available measurements of the pairs (D_m, D_{MAX}), that can be obtained through ADCP, can be used for each reach to calculate $\emptyset$ (W) and W using Eq. (4).

4.2.3 Determination of the maximum depth D_{MAX} :

According to Eq. (4), the determination of D_{MAX} is mainly related to the accurate estimation of the entropy parameter W for each cross-section. However, in situations where the investigation cross-sections are wide, it becomes challenging to determine the value of D_{MAX} without conducting a bathymetric survey. In such cases, if it is assumed that D_{MAX} is completely unknown, it can be estimated based on previous studies. For instance, Moramarco and Singh, (2010) introduced the expression to calculate u_{MAX} for a large river, which depends on (D_{MAX}, W) as:

$$u_{MAX\_cal} = \frac{\sqrt{g\ D_m\ S_f}}{k}\, ln\left[\ \frac{1}{exp(-a\ D_m)}\ \right] \qquad (5)$$

where u_{MAX_Cal} is the calculated maximum velocity in the cross-section, g is the gravitational constant, D_m is the mean depth, k is the constant of Von Kàrmàn for clear water equal to 0.41, S_f is water surface slope, a is a constant which depends on the position where the velocity u=0. Replacing the term of D_m from Eq. (4) in Eq. (5), the formulation of u_{MAX_cal} can be expressed as

$$u_{MAX\_cal} = \frac{\sqrt{g\, D_{MAX} \left(\frac{e^W}{e^W-1}-\frac{1}{W}\right) S_f}}{k} ln\left[\frac{1}{e^{\left[-a\, D_{MAX}\left(\frac{e^W}{e^W-1}-\frac{1}{W}\right)\right]}}\right] \quad (6)$$

The integration of Eq. (6) introduces the variables (D_{MAX}, W) that are also present in Eq. (3), along with other variables (a, S_f). The optimisation of all the variables (D_{MAX}, W, S_f, a) will be performed by minimising the error between the calculated maximum velocity (u_{MAX_cal}) and the observed (u_{MAX}) value in Eq. (3), which is equal to the maximum value of surface velocity over the cross-section ($u_{surf}(x)$).

4.2.4 Optimisation of the variables (W, D_{MAX}, S_f, a):

The Genetic Algorithm solver (GA solver) provided by MATLAB®Optimisation Toolbox (R2019a, The MathWorks Inc., Natick, Massachusetts, USA) is considered an effective optimisation technique used in scientific and engineering problems (Sivanandam et al., 2008). The GA solver is used for the optimisation of the different variables by minimising the following expression:

$$u_{MAX\_cal} - u_{MAX} \leq 10^{-6} \quad (7)$$

The integration of Eq. (6) introduces the variables (D_{MAX}, W) that are also present in Eq. (3), along with other variables (a, S_f). The optimisation of all the variables (D_{MAX}, W, S_f, a) will be performed by minimising the error between the calculated maximum velocity (u_{MAX_cal}) and the observed value in Eq. (3), which is equal to u_{MAX} = max (u_{surf} (x)). The GA solver begins by assigning initial values to variables within their respective

ranges of variability. These parameters are randomly sampled for 1000 initial values. The GA solver iteratively modifies this value until finding the optimal combination that satisfies the conditions stated in Eq. (7). As a result, 1000 bathymetry profiles are generated, from which the 25^{th}, 50^{th}, and 75^{th} percentile profiles can be derived. The process of the estimation of bathymetry and the optimisation of the different variables is presented in Fig. 3. The two scenarios aim to assess the accuracy of the optimisation performed by the genetic algorithm (GA) solver. The key distinction lies in the number of variables used in the optimisation process, as highlighted in step (7) of the figure. Scenario (a) uses four variables (D_{MAX}, W, S_f, a) by considering the entropy parameter W as an unknown, while scenario (b) reduces the variables to three (D_{MAX}, S_f, a) by treating W as a regional parameter estimated through *in-situ* ADCP data. The main objective of this comparative analysis is to examine the estimation of the entropy parameter W, evaluating its performance as both a regional and a calibration parameter to provide insights into the impact of the bathymetry estimation.

4.2.5 Estimation of velocity distribution and mean flow using entropy formulation

The 2D velocity distribution in a river can primarily be determined using Eq. (1) based on the simulated results of bathymetry given by Eq. (3). The accuracy of the flow depth and velocity across the section can be assessed by comparing the profiles obtained from ADCP and the profiles simulated using the entropy theory, as proposed by Bahmanpouri et al. (2022b). The estimation of the mean flow is primarily dependent on two parameters: the results of simulated bathymetry obtained from Eq. (3) for the determination of the flow area and the entropy parameter M for the estimation of the mean velocity. This can be expressed according to Eq. (8):

$$Q_{50^{th}\ \text{Percentile}} = A_{50^{th}\ \text{Percentile}} * u_m \quad (8)$$

315 Where $Q_{50^{th}\ Percentile}$ is the mean flow, $A_{50^{th}\ Percentile}$ is the mean flow area calculated by the
316 integration of the simulated results of bathymetry given by Eq. (3), and u_m is the mean
317 velocity which can be derived based on Eq. (2).

318 **5 Results and discussion**

319 ***5.1 ADCP dataset in the middle reach***

320 Four field campaigns using (ADCP) were carried out on the middle reach of the
321 Congo River during the years 2017, 2019, 2021, and 2022. Transects were selected from
322 these campaigns at evenly distributed locations along a stretch of 1740 km in length,
323 starting from Kisangani to Kinshasa, during both high and low flow seasons. The results
324 obtained from 2022 revealed that the Chenal reach and the Pool Malebo exhibited higher
325 flow velocities compared to the multi-thread reach. These findings were consistent with
326 previous studies in 2017, 2019 and 2021 conducted by Tshimanga et al. (2022a). In
327 particular, the transect in the Pool Malebo (BZ_kin) recorded the highest flow velocity,
328 reaching 2.54 m/s. Regarding the maximum depth, this was observed in the Chanel and
329 the multi-thread reach with a value of 30.5 m. Table 1 provides a summary of the
330 investigation's results for each cross-section.

331 ***5.2 Estimation of the entropy parameters***

332 *5.2.1 Estimation of W through analysis of pairs (D_m, D_{MAX})*

333 The entropy parameter *W* is determined using the observed data of the pairs (*Dm*,
334 D_{MAX}) measured by ADCP in different cross-sections of the middle reach. Due to the
335 limited number of measurements, establishing a robust correlation between the mean and
336 maximum depth (D_m, D_{MAX}) is challenging. However, it is crucial to describe each reach
337 by an entropy parameter *W*. Considering the morphology of the Congo River in the
338 middle reach, it is evident that the Chenal reach varies significantly compared to the Pool

Malebo and the multi-thread reach (Kechnit et al., 2024; Carr et al., 2019). Therefore, a separate W parameter is estimated for each reach of the Congo River, namely the Pool Malebo (Fig. 2 (a)), Chenal (Fig. 2 (b & e)), and multi-thread (Fig. 2 (c&d)), the results are represented in Fig. 4 (a, b and c). The pairs (W, $\emptyset$ (W)) are higher for the Chenal reach in comparison to the other Pool Malebo and Multi-thread reaches. Note, that an increase in the value of W indicates a cross-sectional shape that is more rectangular. However, for larger rivers characterised by irregular bathymetry, the entropy parameter W may assume negative values (Moramarco et al., 2019).

5.2.2 Estimation of M parameter through analysis of pairs (u_m, u_{MAX})

The determination of the entropy parameter M follows a similar approach to that applied for the entropy parameter W. Despite the limited number of measurements available to establish a strong relationship between the pairs (u_m, u_{MAX}), a notable correlation is observed for the middle reach of the Congo River, see Fig. 4 (d). Therefore, M deduced by Eq. (2) and $\emptyset(M)$ can be considered as a parameter that characterises the entire middle reach of the Congo River in the mainstream, with a coefficient of determination R^2 equal to 0.98.

5.3 Estimated bathymetry using the entropy theory

The comparison between the simulated bathymetry at the 50th percentile using the entropy theory scenarios in both scenarios (a) and (b) and the observed profile via ADCP is shown in Fig. 5 respectively for the Pool Malebo, Chenal and Multi-thread reaches. Other results are represented in the Supplementary material, (see Figures S2, S3 and S4). The grey area represents the 1000 bathymetry profiles generated by the GA Solver according to the initial value of the parameters (D_{MAX}, W, S_f, a) that are randomly sampled. The coefficient of correlation is calculated for each cross-section, as follows:

- R1 is the correlation between the 50th percentile of the simulated bathymetry (scenario a) and the observed profile via ADCP.
- R2 is the correlation between the 50th percentile of the simulated bathymetry (scenario b) and the observed profile via ADCP.
- R3 is the correlation between the 50th percentile of the simulated bathymetry (scenario a) and (scenario b).

A good correlation was observed in the Chanel, specifically in the Maluku and Kisangani transects, with correlation coefficients ranging from 0.68 to 0.88. The bathymetry in this reach displayed a rectangular shape. Additionally, a high correlation coefficient of 0.99 was observed between the estimated bathymetry with the observed one in scenarios (a, b). Indeed, when the entropic parameter W was used as a calibration parameter (scenario a), the profile exhibited a closer resemblance to the measured profile via ADCP. Furthermore, the trend in the multi-thread was found to be higher compared to the Pool Malebo, with correlation coefficients varying from 0.57 to 0.84 and 0.49 to 0.71, respectively.

It is worth noting that the bathymetry in the Pool Malebo and multi-thread reaches respectively in Fig. 5 and (see Supplementary material, Figure S1 and S4) differs from the Chenal reach in Fig. 5 (see Supplementary material, Figure S3). For Pool Malebo, the flow velocity is low and the distance between the two banks is large, which allows for the deposition of sand bars, explaining the irregularity of the bathymetry in this reach. However, the estimated results using the entropy theory yielded a strong correlation with the measured ones. The difference between the 50th percentile of the estimated results in both scenarios (a, b) is not significant. Furthermore, a strong correlation is observed in all the transects of investigation. In the process of optimisation, the performance of a

387 genetic algorithm (GA) solver depends on the number of variables used in the
388 optimisation problem, which is the key difference between scenarios (a) and (b). In
389 scenario (a), the introduction of the entropy parameter W makes the problem more
390 complex. However, it also shows the advantage of using additional variables, which can
391 lead to more accurate and robust solutions.

392 Fig. 6 presents the range of variability for the different parameters (D_{MAX}, W, S_f,
393 a) used in the optimisation process by GA Solver for both scenarios (a, b). Three transects
394 from each reach are chosen, respectively Pool Malebo, Chenal, and Multi-thread. In
395 particular, the choice of whether the entropy parameter W is treated as a calibration or
396 regional parameter that is derived by measurements of the pairs (D_m, D_{MAX}) has a
397 significant impact on the variability of the other parameters, as illustrated in Fig. 6. The
398 restricted number of measurements obtained from the pairs (D_m, D_{MAX}) introduces a
399 significant amount of uncertainty regarding the value of W in scenario (a). Nonetheless,
400 this approach might be suitable in large rivers such as the Congo for the regionalisation
401 of the parameter W where there is a complete lack of ground-based historical observations
402 and regular field measurements due to accessibility and technical resources problems,
403 especially during high flow periods (Washington et al., 2013).

404 ***5.4 Entropy-based analysis of 2D velocity distribution***

405 The use of Eq. (1) for the analysis of the 2D velocity distribution is primarily
406 based on the results of the simulated bathymetry obtained from the application of Eq. (3)
407 and the determination of the M value suggested by Eq. (2). A comparison of the velocity
408 distribution obtained through ADCP and using the entropy theory is represented in Fig. 7
409 for the Maluku transect (Chenal reach).

410 In order to compare the estimated profile obtained through the entropy theory with
411 the observed profile obtained via ADCP, the approach proposed by Bahmanpouri et al.,

(2022b) is adopted. The ADCP velocity data are collected at multiple points across the cross-section and analysed using Dplot® software (Hydesoft Computing, LLC), which enables the generation of a continuous, two-dimensional velocity profile spanning the entire cross-section. This is achieved by interpolating the ADCP data points at consistent intervals along both the horizontal (x) and vertical (y) axes, ensuring that the resulting velocity profile has no gaps and providing a detailed two-dimensional representation of the flow velocity from the water surface to the bed.

The estimated velocity profile is computed based on the simulated bathymetry from the entropy model and collected surface velocity by ADCP. The velocity data is interpolated at regular 1 m intervals along the (x, y) coordinates to generate an error dataset. However, it is important to note that the estimated bathymetry profile may not accurately represent the actual depth due to variations in correlation along each transect. The error dataset is determined by comparing the two velocity profiles, where a 100% error indicates either an error in water depth or in the blanking zone where the ADCP does not provide velocity values. Fig. 7 shows that the error in the velocity profile remains within 15% in areas where the two profiles overlap. However, the error increases near the blanking zone close to the bed, which is an area where acoustic reflections from the bed interfere with the ADCP measurements. The obtained results are highly satisfactory and show a remarkable similarity to the observations made by the ADCP. Further velocity data analyses are represented in the Supplementary material (see Figures S5, S6 and S7)

5.5 Discharge assessment using entropy theory

Table 2 presents a comparative analysis between the 50^{th} percentile simulated parameters of flow, flow area, and mean velocity obtained using entropy theory and the corresponding observed values obtained via ADCP in all transects of the middle reach spanning over 1740 km.

In order to enhance the analysis of the errors observed in discharge, flow area, and mean velocity, histograms with a normal distribution were fit and are shown in Fig. 8. The errors observed in all parameters exhibit both positive and negative values. The range of variability is between -30% to 35% for the discharge, -40% to 45% for the flow area, and -25% to 30% for the mean velocity. Additionally, the standard deviation for the error for discharge, flow area and mean velocity are respectively 18 %, 17% and 12%, which is not above ± 20%.

5.6 Error variability distribution and uncertainty analysis

The analysis of the error dataset is crucial for understanding the quality and reliability of the results provided by the entropy theory. One important aspect to consider is studying the variability pattern of the errors. By thoroughly examining the distribution, statistical properties, and relationships of the errors, we can gain valuable insights into the performance and accuracy of the approach. In this study, a graphical method known as a Quantile-Quantile (QQ) plot is used to analyse the errors in both discharge and flow areas. This plot compares the observed errors with those expected from a normal distribution (see Fig. 9).

From Fig. 9, it is evident that the magnitudes closely adhere to a straight line, for both discharge and flow area, indicating a normal distribution of the error. To confirm these results, additional statistical tests are employed. In this regard, common goodness-of-fit tests for normal distribution, as outlined by Öner and Kocakoç (2017), are used (see Table 3).

According to Table 3, the statistics test value falls between 0 and 1, and their interpretation depends on the specific test and the context of analysis. In the case of Kolmogorov-Smirnov and Anderson-Darling, the statistic test measures the maximum difference between the empirical distribution of the dataset and the normal distribution.

A statistics test value closer to 0 indicates a better fit to a normal distribution. On the other hand, for the Shapiro-Wilk test, the statistic test value represents the correlation between the observed and expected normal distribution, a higher value suggests that the data is more likely to follow a normal distribution.

Based on the p-values obtained from tests (Kolmogorov-Smirnov, Anderson-Darling, and Shapiro-Wilk), it is noted that the value exceeds the alpha level of $\alpha = 0.05$. This finding further supports the notion that the error data set is normally distributed. The normality of the error between the estimated and observed results for both discharge and flow area indicates that a majority of the data points are clustered near the mean values equal to 1.3% and 2.7%, respectively. These numbers are quite close to zero, indicating that the simulated and observed results are fairly similar.

6 Conclusions

This study demonstrates, for the first time, the successful application of an entropy-based approach to estimate bathymetry and discharge in large rivers. The method lends itself well to monitoring inland waters using ground satellite-based platforms where no information on river topography is available and/or the sampling of velocity is not always feasible across the whole flow area, especially in braided and multi-thread reaches.

Despite the limited number of measurements for the estimation of *W*, a good correlation can be observed between the simulated bathymetry in both scenarios, (a) universal *W* and (b) reach-based *W,* and the observations over a 1740 km reach at 29 cross-sections. The trend of the simulated bathymetry results closely resembles the observed bathymetry when the cross-section shape is close to rectangular, as seen in the Chenal reach. For example, the correlation decreases when the bathymetry becomes more irregular in the Pool Malebo. Additionally, a strong correlation is found between the

simulated results in both scenarios (a) and (b), even though W is estimated with two different approaches. These findings validate the effectiveness of GA solver optimisation and identify a novel aspect of entropy application in using W as a regional parameter for the bathymetry, based on the river channel morphology.

The approach enables the determination of the 2D cross-sectional velocity distribution based on the simulated bathymetry results. The error observed is less than 20% when the simulated and the observed velocity profiles of cross-sections are compared, with a slightly higher error value near the blanking zone. This finding is consistent with the study of Bahmanpouri et al. (2022b), where they used an entropy approach based on ADCP data and found an error of no more than 15% in the predicted 2D velocity distribution, while the bathymetry data was considered as an observed quantity. The entropy method has proven to be effective in discharge monitoring, providing a reliable result with an average error not exceeding 2.7% in challenging environments such as the Congo River. This finding aligns with other results from studies that have also used the entropy approach for discharge assessment. For instance, Bahmanpouri et al. (2022a) reported an error rate not exceeding 13%, while Vyas et al. (2020) used both the Shannon and Tsallis approaches and achieved an average not exceeding 10%. However, this is the first time it has been demonstrated successfully for a very large river.

The entropy-based approach, which was tested for large rivers such as the Congo in this study, offers a valuable tool for monitoring discharge by sampling only a few surface velocities across the river. This approach has significant implications for remote sensing applications, particularly in ungauged large river basins. Moramarco et al. (2019) found that using satellite observations to estimate discharge rates resulted in an average error percentage of approximately 30%. This was achieved by combining data from

MODIS optical and radar altimetry for the surface water level. Recent findings by Everard et al. (2023), Masafu et al. (2023), and Masafu and Williams (2024) demonstrated that measuring surface flow velocity in medium and large rivers is possible using high-resolution satellite video. Combining a satellite velocity estimate with the entropy-based method, demonstrated here, could lead to a new none-contact method for monitoring large river basins. Further research in this context would be of great interest in future studies, expanding on the work presented here.

Overall, the application of entropy theory in estimating bathymetry in large rivers, such as the Congo, holds significant promise. By incorporating this data into hydraulic models, a more comprehensive understanding of river dynamics and hydraulics can be achieved. Additionally, further research on the integration of entropy theory with hydraulics models, particularly in the context of navigation, is still necessary. This is especially crucial considering the growing number of accidents and fatalities during navigation in the Congo River, highlighting the importance of exploring entropy theory's potential with hydraulic models for developing navigation maps and enhancing safety.

Acknowledgements

The field measurements were conducted by the Congo Basin Water Resources Research Center (CRREBaC), Congo River Authority (RVF) in DR Congo, and the CRuHM project team. The authors would like to express their gratitude to these organisations for providing all the necessary data for this research.

Funding details

KECHNIT Djamel was supported by the Intra-African Academic Mobility Scheme of the European Union, under the African Water Resources Mobility Network (AWaRMN) program No. 2019-1973/004-001 and GERNAC/CICOS project under the GMES & AFRICA II program. Mark Trigg, Andrew Carr and Raphael Tshimanga were supported

by the Royal Society CRISP project, under the Africa Capacity Building Initiative (FLR\R1\192057 and FCG\R1\201027).

Disclosure statement

The authors report there are no competing interests to declare.

Data availability

The data used in this study is available on request from the corresponding author.

References

Alsdorf, D., Beighley, E., Laraque, A., Lee, H., Tshimanga, R., O'Loughlin, F., Mahé, G., Dinga, B., Moukandi, G., Spencer, R.G.M., 2016. Opportunities for hydrologic research in the Congo Basin. Rev. Geophys. 54, 378–409. https://doi.org/10.1002/2016RG000517

Ammari, A., Remini, B., 2010. Estimation of Algerian rivers discharges based one Chiu's equation. Arab. J. Geosci. 3, 59–65. https://doi.org/10.1007/s12517-009-0056-y

Ammari, A., Moramarco, T., Meddi, M., 2017. A simple entropy-based method for discharges measurements in gauged and ungauged river sites: the case study of coastal Algerian river. Bull. L'Institut Sci. Rabat 39, 35–44.

Ammari, A., Bahmanpouri, F., Khelfi, M.E.A., Moramarco, T., 2022. The regionalizing of the entropy parameter over the north Algerian watersheds: a discharge measurement approach for ungauged river sites. Hydrol. Sci. J. 67, 1640–1655. https://doi.org/10.1080/02626667.2022.2099744

Bahmanpouri, F., Eltner, A., Barbetta, S., Bertalan, L., Moramarco, T., 2022a. Estimating the average river cross-section velocity by observing only one surface velocity value and calibrating the entropic parameter. Water Resources Research, https://doi.org/10.1029/2021WR031821

Bahmanpouri, F., Barbetta, S., Gualtieri, C., Ianniruberto, M., Filizola, N., Termini, D., Moramarco, T., 2022b. Prediction of river discharges at confluences based on Entropy theory and surface-velocity measurements. J. Hydrol. 606, 127404. https://doi.org/10.1016/j.jhydrol.2021.127404

Bates, P.D., Tshimanga, R., Trigg, M.A., Carr, A., Mushi, C.A., Kabuya, P.M., Bola, G., Neal, J., Ndomba, P., Mtalo, F., Hughes, D., 2024. Creating sustainable capacity

for river science in the Congo basin through the CRuHM project. Interface Focus. https://doi.org/10.1098/rsfs.2023.0079

Carr, A. B., Trigg, M. A., Tshimanga, R. M., Borman, D. J., & Smith, M. W. 2019. Greater water surface variability revealed by new Congo River field data: Implications for satellite altimetry measurements of large rivers. Geophysical Research Letters, 46, 8093– 8101. https://doi.org/10.1029/2019GL083720

Carr, A.B., Trigg, M.A., Tshimanga, R.M., Smith, M.W., Borman, D.J. and Bates, P.D. (2022). Estimation of Bathymetry for Modeling Multi-thread Channel Hydraulics. In Congo Basin Hydrology, Climate, and Biogeochemistry (eds R.M. Tshimanga, G.D.M. N'kaya and D. Alsdorf). https://doi.org/10.1002/9781119657002.ch15

Chiu, C.-L., 1987. Entropy and Probability Concepts in Hydraulics. J. Hydraul. Eng. 113, 583–599. https://doi.org/10.1061/(ASCE)0733-9429(1987)113:5(583)

Chiu, C.-L., 1988. Entropy and 2-D Velocity Distribution in Open Channels. J. Hydraul. Eng. 114, 738–756. https://doi.org/10.1061/(ASCE)0733-9429(1988)114:7(738)

Chiu, C.-L., 1989. Velocity Distribution in Open Channel Flow. J. Hydraul. Eng. 115, 576–594. https://doi.org/10.1061/(ASCE)0733-9429(1989)115:5(576)

CICOS. (2023). International Commission of the Congo-Oubangui- Sangha Basin (CICOS): Voies Navigables. Available at: https://www.cicos.int/navigation-interieure/ voies-navigables/

Everard, N., Dixon, H., Sarkar, S., Randall, M., and Schumann, G.: The FluViSat project: Measuring stream flow from space with very high-resolution Planet satellite video, EGU General Assembly 2023, Vienna, Austria, 24–28 Apr 2023, EGU23-1374, https://doi.org/10.5194/egusphere-egu23-1374

Gaye, C.B., Tindimugaya, C., 2019. Challenges and opportunities for sustainable groundwater management in Africa. Hydrogeol. J. 27, 1099–1110. https://doi.org/10.1007/s10040-018-1892-1

Gebrehiwot, S.G., Ellison, D., Bewket, W., Seleshi, Y., Inogwabini, B.-I., Bishop, K., 2019. The Nile Basin waters and the West African rainforest: Rethinking the boundaries. WIREs Water 6, e1317. https://doi.org/10.1002/wat2.1317

Jung, H.C., Hamski, J., Durand, M., Alsdorf, D., Hossain, F., Lee, H., Hossain, A.K.M.A., Hasan, K., Khan, A.S., Hoque, A.K.M.Z., 2010. Characterization of complex fluvial systems using remote sensing of spatial and temporal water level variations

in the Amazon, Congo, and Brahmaputra Rivers. Earth Surf. Process. Landf. 35, 294–304. https://doi.org/10.1002/esp.1914

Kechnit, D., Tshimanga, R.M., Ammari, A., Trigg, M., 2024. Assessing Uncertainties of a Remote Sensing-based Discharge Reflectance Model for Applications to Large Rivers of the Congo Basin. Hydrol. Sci. J. https://doi.org/10.1080/02626667.2024.2378486

Kim, D., Yu, H., Lee, H., Beighley, E., Durand, M., Alsdorf, D.E., Hwang, E., 2019. Ensemble learning regression for estimating river discharges using satellite altimetry data: Central Congo River as a Test-bed. Remote Sens. Environ. 221, 741–755. https://doi.org/10.1016/j.rse.2018.12.010

Legleiter, C.J., Kinzel, P.J., 2021. Surface Flow Velocities from Space: Particle Image Velocimetry of Satellite Video of a Large, Sediment-Laden River. Front. Water 3. https://doi.org/10.3389/frwa.2021.652213

Legleiter, C.J., Kinzel, P.J., Laker, M., Conaway, J.S., 2023. Moving Aircraft River Velocimetry (MARV): Framework and Proof-of-Concept on the Tanana River. Water Resour. Res. 59, e2022WR033822. https://doi.org/10.1029/2022WR033822

Masafu, C., Williams, R., Shi, X., Yuan, Q., Trigg, M., 2022. Unpiloted Aerial Vehicle (UAV) image velocimetry for validation of two-dimensional hydraulic model simulations. J. Hydrol. 612, 128217. https://doi.org/10.1016/j.jhydrol.2022.128217

Masafu, C., Williams, R., Hurst, M.D., 2023. Satellite Video Remote Sensing for Estimation of River Discharge. Geophys. Res. Lett. 50, e2023GL105839. https://doi.org/10.1029/2023GL105839

Masafu, C., Williams, R., 2024. Satellite Video Remote Sensing for Flood Model Validation. Water Resour. Res. 60, e2023WR034545. https://doi.org/10.1029/2023WR034545

Mitchell, S.A., 2013. The status of wetlands, threats and the predicted effect of global climate change: the situation in Sub-Saharan Africa. Aquat. Sci. 75, 95–112. https://doi.org/10.1007/s00027-012-0259-2

Moramarco, T., Saltalippi, C., Singh, V., 2004. Estimation of Mean Velocity in Natural Channels Based on Chiu's Velocity Distribution Equation. J. Hydrol. Eng. - J HYDROL ENG 9. https://doi.org/10.1061/(ASCE)1084-0699(2004)9:1(42)

633 Moramarco, T., Singh, V.P., 2010. Formulation of the Entropy Parameter Based on
634 Hydraulic and Geometric Characteristics of River Cross Sections. J. Hydrol. Eng.
635 15, 852–858. https://doi.org/10.1061/(ASCE)HE.1943-5584.0000255
636 Moramarco, T., Saltalippi, C., Singh, V.P., 2011. Velocity profiles assessment in natural
637 channels during high floods. Hydrol. Res. 42, 162–170.
638 http://dx.doi.org/10.2166/nh.2011.064
639 Moramarco, T., Corato, G., Melone, F., Singh, V.P., 2013. An entropy-based method for
640 determining the flow depth distribution in natural channels. J. Hydrol. 497, 176–
641 188. https://doi.org/10.1016/j.jhydrol.2013.06.002
642 Moramarco, T., Barbetta, S., Tarpanelli, A., 2017. From Surface Flow Velocity
643 Measurements to Discharge Assessment by the Entropy Theory. Water 9, 120.
644 https://doi.org/10.3390/w9020120
645 Moramarco, T., Barbetta, S., Bjerklie, D.M., Fulton, J.W., Tarpanelli, A., 2019. River
646 Bathymetry Estimate and Discharge Assessment from Remote Sensing. Water
647 Resour. Res. 55, 6692–6711. https://doi.org/10.1029/2018WR024220
648 O'Loughlin, F.E., Neal, J., Schumann, G.J.P., Beighley, E., Bates, P.D., 2020. A
649 LISFLOOD-FP hydraulic model of the middle reach of the Congo. J. Hydrol. 580,
650 124203. https://doi.org/10.1016/j.jhydrol.2019.124203
651 Öner, M., Kocakoç, İ. D., 2017.A Compilation of Some Popular Goodness of Fit Tests
652 for Normal Distribution: Their Algorithms and MATLAB Codes (MATLAB).
653 JMASM 49, 16(2), 547-575. https://10.22237/jmasm/1509496200
654 Patel, P., Sarkar, A., 2023. Streamflow Estimation Using Entropy-Based Flow Routing
655 Technique in Brahmani River, Odisha, in: Pandey, M., Gupta, A.K., Oliveto, G.
656 (Eds.), River, Sediment and Hydrological Extremes: Causes, Impacts and
657 Management, Disaster Resilience and Green Growth.Nat.Singap, Singapore, pp.
658 167–182. https://doi.org/10.1007/978-981-99-4811-6_9
659 Revel, M., Yamazaki, D., Kanae, S., 2018. Estimating Global River Bathymetry by
660 Assimilating Synthetic SWOT Measurements. Annu. J. Hydraul. Eng. JSCE, 74,
661 I_307–I_312 https://doi.org/10.2208/jscejhe.74.I_307
662 Runge, J., 2022. The Congo River, Central Africa, in: Large Rivers. John Wiley & Sons,
663 Ltd, pp. 433–456. https://doi.org/10.1002/9781119412632.ch15
664 Schumann, G. and Everard, N. 2022. FluViSat: Technical Note on the Opportunities for
665 EO Services. Available from: https://www.ceh.ac.uk/sites/default/files/2022-
666 12/technical-note-EO-services-opportunties-FluViSat.pdf

667 Sivanandam, S., Deepa, S. 2008. Genetic Algorithm Implementation Using Matlab. In:
668 Introduction to Genetic Algorithms. Springer, Berlin, Heidelberg.
669 https://doi.org/10.1007/978-3-540-73190-0_8
670 Singh, G., Khosa, R., 2023. Application of the Kapur entropy for two-dimensional
671 velocity distribution. Stoch Environ Res Risk Assess 37, 3585–3598.
672 https://doi.org/10.1007/s00477-023-02464-7
673 Termini, D., Moramarco, T., 2016. Application of entropic approach to estimate the mean
674 flow velocity and Manning roughness coefficient in a high-curvature flume.
675 Hydrol. Res. 48, 634–645. https://doi.org/10.2166/nh.2016.106
676 Trigg, M.A., Tshimanga, R.M., 2020. Capacity Building in the Congo Basin: Rich
677 Resources Requiring Sustainable Development. One Earth 2, 207–210.
678 https://doi.org/10.1016/j.oneear.2020.02.008
679 Trigg, M., Carr, A., Tshimanga, R., Mokango, G., Yamazaki, D., Frasson, R. P., &
680 Rodriguez, E. 2021. High resolution hydrodynamic modelling of the Congo River
681 combining field data, remote sensing and partnership. In AGU Fall Meeting
682 Abstracts (Vol. 2021, pp. H12I-03).
683 Trigg, M.A., Carr, A.B., Smith, M.W. and Tshimanga, R.M. 2022a. Measuring
684 Geomorphological Change on the Congo River Using Century-Old Navigation
685 Charts. In Congo Basin Hydrology, Climate, and Biogeochemistry (eds R.M.
686 Tshimanga, G.D.M. N'kaya and D. Alsdorf).
687 https://doi.org/10.1002/9781119657002.ch21
688 Trigg, M.A., Tshimanga, R.M., Ndomba, P.M., Mtalo, F., Hughes, D.A., Mushi, C.A.,
689 Bola, G.B., Kabuya, P.M., Carr, A.B., Bernhofen, M., Neal, J., Beya, J.T.,
690 Ngandu, F.K. and Bates, P.D. 2022b. Putting River Users at the Heart of
691 Hydraulics and Morphology Research in the Congo Basin. In Congo Basin
692 Hydrology, Climate, and Biogeochemistry (eds R.M. Tshimanga, G.D.M. N'kaya
693 and D. Alsdorf). https://doi.org/10.1002/9781119657002.ch28
694 Tshimanga, R.M. 2022. Two Decades of Hydrologic Modeling and Predictions in the
695 Congo River Basin. In: R.M. Tshimanga, G.D.M. N'kaya and D. Alsdorf (Eds).
696 Congo Basin Hydrology, Climate, and Biogeochemistry.
697 https://doi.org/10.1002/9781119657002.ch12
698 Tshimanga, R.M., Trigg, M.A., Neal, J., Ndomba, P.M., Hughes, D.A., Carr, A.B.,
699 Kabuya, P.M., Bola, G.B., Mushi, C.A., Beya, J.T., Ngandu, F.K., Mokango,
700 G.M., Mtalo, F. and Bates, P.D. 2022a. New Measurements of Water Dynamics

and Sediment Transport along the Middle Reach of the Congo River and the Kasai Tributary. In Congo Basin Hydrology, Climate, and Biogeochemistry (eds R.M. Tshimanga, G.D.M. N'kaya and D. Alsdorf). https://doi.org/10.1002/9781119657002.ch23

Tshimanga, R.M., N'kaya, G.D.M., Laraque, A., Nicholson, S.E., Onema, J.-M.K., Lumbuenamo, R. and Alsdorf, D. 2022b. Congo Basin Research. In Congo Basin Hydrology, Climate, and Biogeochemistry (eds R.M. Tshimanga, G.D.M. N'kaya and D. Alsdorf). https://doi.org/10.1002/9781119657002.ch1

Tshimanga, R.M., Bola, G.B., Kabuya, P.M., Nkaba, L., Neal, J., Hawker, L., Trigg, M.A., Bates, P.D., Hughes, D.A., Laraque, A., Woods, R. and Wagener, T. 2022c. Towards a Framework of Catchment Classification for Hydrologic Predictions and Water Resources Management in the Ungauged Basin of the Congo River. In Congo Basin Hydrology, Climate, and Biogeochemistry (eds R.M. Tshimanga, G.D.M. N'kaya and D. Alsdorf). https://doi.org/10.1002/9781119657002.ch24

Vyas, J.K., Perumal, M., Moramarco, T., 2020. Discharge Estimation Using Tsallis and Shannon Entropy Theory in Natural Channels. Water 12, 1786. https://doi.org/10.3390/w12061786

Washington, R., James, R., Pearce, H., Pokam, W.M., Moufouma-Okia, W., 2013. Congo Basin rainfall climatology: can we believe the climate models? Philos. Trans. R. Soc. B Biol. Sci. 368, 20120296. https://doi.org/10.1098/rstb.2012.0296

Table 1. Hydraulic parameters observed in the data acquisition using ADCP over 1740 km in the middle reach of the Congo River: Chainage from River authority RFV gauge station (C), Number of transect (N), width of transect (L), mean depth (D_m), Maximum depth (D_{MAX}), flow area (A), flow (Q), Mean velocity (u_m), maximum velocity (u_{MAX})

Order of River	Date	Transect	C (km)	N	L (m)	D_m (m)	D_{MAX} (m)	A (m^2)	Q (m^3/s)	u_m (m/s)	u_{MAX} (m/s)
Main course (Pool Malebo)	21/12/2021	BZ_Kin	0	1	3671	11	20.8	40417	52650	1.3	2.57
	23/05/2021			2	3548	10.7	20.1	37832	43043	1.14	2.27
	24/05/2021	Kin_Island	1.5	3	3504	10.8	22.1	37826	44310	1.17	2.37
	25/07/2022	Pool_2	4.5	4	3679	6	12.4	22000	26279	1.19	2.45
	27/07/2022	Ndjili	9	5	2042	14.4	22.7	29323	22057	0.75	2.06
Main course (Chenal)	21/05/2021		45	6	5565	6.9	17.2	38646	39711	1.03	2.07
	20/05/2021	Maluku	53	7	2976	12.1	18.9	35934	43131	1.2	1.94
	20/05/2021		60	8	2341	15.8	26.4	36914	43642	1.18	2.42
	30/07/2017	Kunzulu	155	9	1646	15.3	24	25254	28649	1.13	2.4
	03/08/2017	Kwamouth	190	10	1925	12.2	30.5	23435	29326	1.25	2.53
	03/08/2017	Lenga	195	11	1858	13.1	21.8	24304	22515	0.93	1.73
Tributary	04/08/2017	Kasai	193	12	623	12.2	14.2	7585	7395	0.97	1.81
Main Course (Multi-thread)	09/08/2017	Lukolela	250	13	1847	11	25.4	20276	19687	0.97	2.03
	10/08/2017	Clocke point	540	14	6352	3.8	16.4	24151	20655	0.86	2.24
	13/08/2017	Gombe	580	15	2676	11.3	30.5	30272	22609	0.75	1.78
Tributary	16/08/2019	Ruki	700	16	602	7.4	10.4	4458	2997	0.67	1.34
	13/08/2019	Lulonga	770	17	638	3.6	4.51	2318	1653	0.71	1.58
Main Course (Multi-thread)	12/08/2019	Makanza	900	18	2992	4	9.7	11829	8517	0.72	1.45
	13/08/2019			19	1126	4.6	8.86	5165	2970	0.58	1.3
	07/08/2019	Bumba		20	1664	3.2	6.53	5310	3877	0.73	1.34
	08/08/2019		1340	21	301	2.8	7.1	850	591	0.7	1.13
	09/08/2019			22	1793	3.8	8.9	6880	5126	0.75	1.4
	05/08/2019	Mombongo	1450	23	3586	3.7	7.04	13337	9569	0.72	1.84
	04/08/2019	Lokutu	1530	24	3002	4	8.7	12080	7589	0.63	1.28
Tributary	04/08/2019	Arumimi	1370	25	495	4.9	9.62	2446	1807	0.74	1.46
Main Course (Multi-thread)	03/08/2019	Lileko	1590	26	1850	4.6	13.8	8484	7602	0.9	1.67
Tributary	01/08/2019	Lomami	1620	27	664	2.5	7.76	1669	1135	0.68	1.69
	01/08/2019	Isangi	1615	28	1564	3.2	5.55	5060	840	0.17	1.19
Main Course (Chenal)	28/07/2019	Kisangani	1740	29	783	5.9	11.6	4602	4975	1.08	2.47

Table 2. Comparison between the observed and the estimated parameters using the entropy theory: A (m^2) flow area, Q (m^3/s) discharge, U_m (m/s) mean velocity

Transect	50^{th} Percentile Simulated by Entropy			Observed by ADCP			Error (%)		
	$A_{50^{th}}$	Q	U_m	A	Q	U_m	A	Q	Um
	(m^2)	(m^3/s)	(m/s)	(m^2)	(m^3/s)	(m/s)			
BZ_kin	43358	52595	1.21	40417	52650	1.3	7.30%	-0.10%	-6.90%
	39662	42495	1.07	37832	43043	1.14	4.80%	-1.30%	-6.10%
Kin Island	40606	45423	1.12	37826	44310	1.17	7.30%	2.50%	-4.30%
Pool_2	23963	27711	1.16	22000	26279	1.19	8.90%	5.40%	-2.50%
Ndjili	25240	24518	0.97	29323	22057	0.75	-13.90%	11.20%	29.30%
Maluku	44468	43405	0.98	38646	39711	1.03	15.10%	9.30%	-4.90%
	36767	33615	0.91	35934	43131	1.2	2.30%	-22.10%	-24.20%
	39324	44917	1.14	36914	43642	1.18	6.50%	2.90%	-3.40%
Kunzulu	24221	27403	1.13	25254	28649	1.13	-4.10%	-4.30%	0.00%
Kwamouth	27243	32533	1.19	23435	29326	1.25	16.20%	10.90%	-4.80%
Lenga	21610	17666	0.82	24304	22515	0.93	-11.10%	-21.50%	-11.80%
Kasai	6408	5465	0.85	7585	7395	0.97	-15.50%	-26.10%	-12.40%
Lukolela	26944	25753	0.96	20276	19687	0.97	32.90%	30.80%	-1.00%
Cock point	29304	27663	0.94	24151	20655	0.86	21.30%	33.90%	9.30%
Gombe	20385	18281	0.9	30272	22609	0.75	-32.70%	-19.10%	20.00%
Ruki	4191	2643	0.63	4458	2997	0.67	-6.00%	-11.80%	-6.00%
Lulonga	2284	1707	0.75	2318	1653	0.71	-1.50%	3.30%	5.60%
Makanza	14573	10001	0.69	11829	8517	0.72	23.20%	17.40%	-4.20%
	5758	3525	0.61	5165	2970	0.58	11.50%	18.70%	5.20%
Bumba	4483	2844	0.63	5310	3877	0.73	-15.60%	-26.60%	-13.70%
	6953	4598	0.66	6880	5126	0.75	1.10%	-10.30%	-12.00%
Mombongo	12824	11131	0.87	13337	9569	0.72	-3.80%	16.30%	20.80%
Lokutu	9067	5478	0.6	12080	7589	0.63	-24.90%	-27.80%	-4.80%
Arumimi	2495	1724	0.69	2446	1807	0.74	2.00%	-4.60%	-6.80%
Lileko	12373	9770	0.79	8484	7602	0.9	45.80%	28.50%	-12.20%
Lomami	1363	1084	0.8	1669	1135	0.68	-18.30%	-4.50%	17.60%
Kisangani	5259	6126	1.16	4602	4975	1.08	14.30%	23.10%	7.40%

Table 3. Normality test for the error distribution in discharge and flow area, indicating 0 for non-normal error distribution and 1 for normal error distribution.

Test Name	Discharge [Q m^3/s]			Flow Area [A m^2]			Normality
	Test Statistic	p-value	α	Test Statistic	p-value	α	[0, 1]
Kolmogorov-Smirnov	0.482	0.974	0.05	0.371	0.999	0.05	1
Anderson-Darling	0.244	0.765	0.05	0.156	0.954	0.05	1
Shapiro-Wilk	0.964	0.463	0.05	0.988	0.988	0.05	1

List of figures captions

Figure 1. The Congo River Basin network

Figure 2. ADCP transect investigation over 1740 km in the middle reach of the Congo River starting from Kinshasa to Kisangani: (a) Pool Malebo & Maluku section; (b) Confluence of Kasai tributary in the Congo River; (c) Multi-thread channel between Lukolela and Gombe; (d) Bumba transect; (e) Kisangani (river course from Landsat 8_9, source: https://earthexplorer.usgs.gov/)

Figure 3. Process of the estimation of bathymetry using entropy theory: scenario (a) all the variables are optimised by GA solver, scenario (b): W is estimated based on measurements of (D_m, D_{MAX}) using ADCP.

Figure 4. Linear relationship between the mean and the maximum depth in the (a) Pool Malebo, (b) Chenal and (c) multi-thread reaches, (d) Linear Relationship between the mean and the maximum velocity in all the cross-section of the middle reach of the Congo River.

Figure 5. Comparison of 50^{th} estimated bathymetry using the entropy theory and measured profile using ADCP in the different transect of the middle reach of the Congo River, Correlation analysis is presented in (R1, R2, R3).

Figure 6. Boxplot of the range of variability of the different parameter (D_{MAX}, S_f, a, W) optimised by GA solver for 1000 realizations in both scenarios where scenario (a): W is estimated by GA solver, scenario (b) W is estimated based on measurements of (D_m, D_{MAX}).

Figure 7. Velocity distribution in 2D using the entropy theory where the simulated bathymetry is used with error percentage dataset for the Maluku_2 transect compared to the observed via ADCP data.

Figure 8. Histogram of the error data set for the different parameters with a normal fit distribution.

Figure 9. QQ Plot of sample data versus normal for the error between the estimated and observed results for both discharge and flow area.

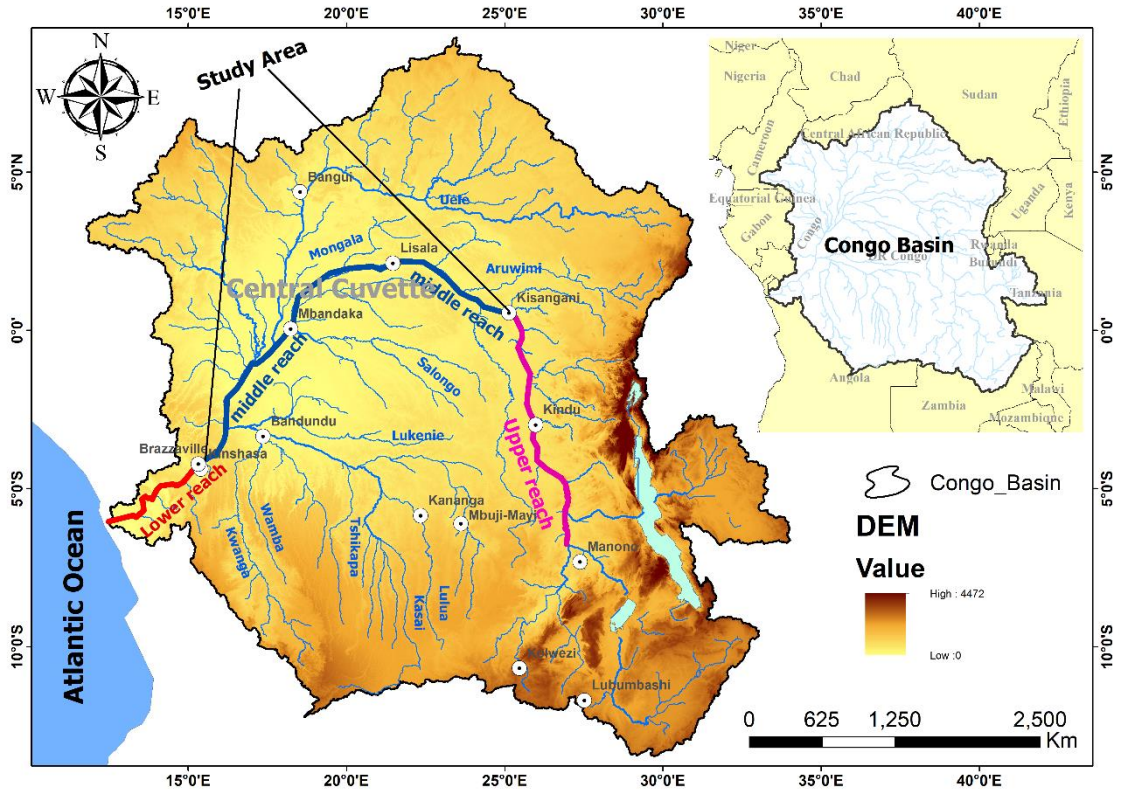

Figure 1. The Congo River Basin network

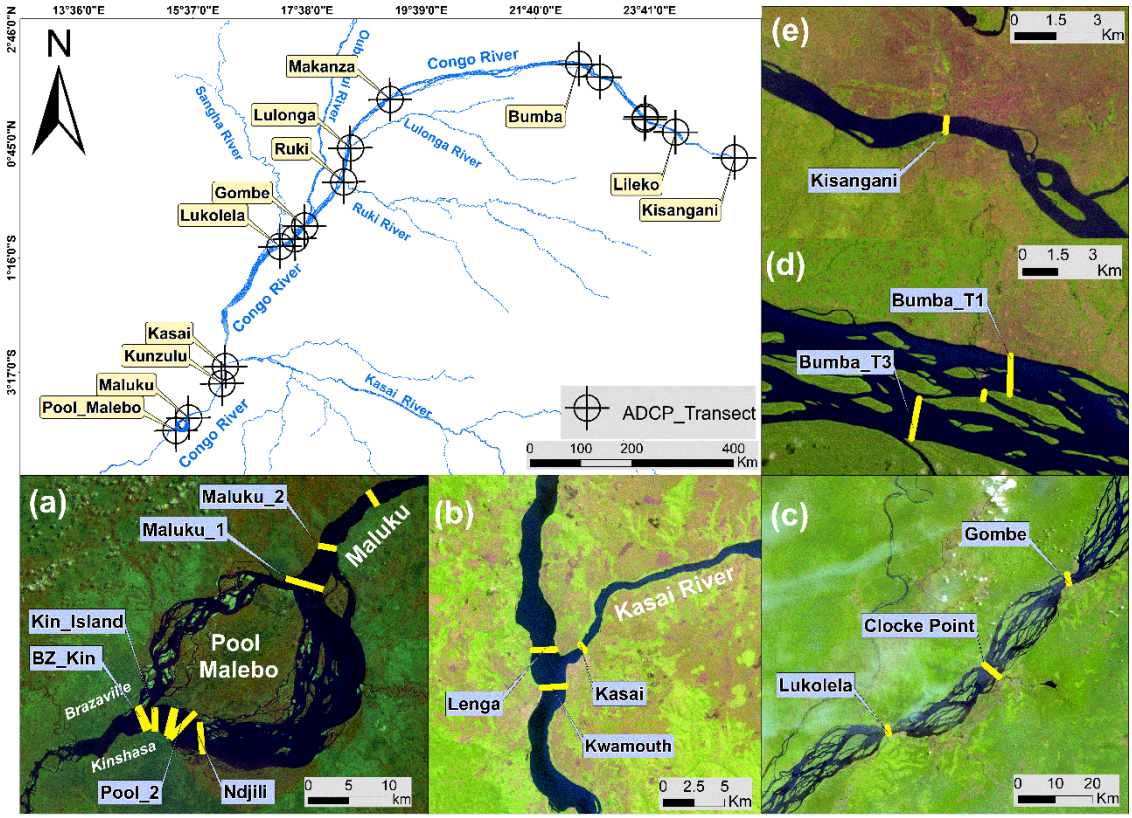

Figure 2. ADCP transect investigation over 1740 km in the middle reach of the Congo River starting from Kinshasa to Kisangani: (a) Pool Malebo & Maluku section; (b) Confluence of Kasai tributary in the Congo River; (c) Multi-thread channel between Lukolela and Gombe; (d) Bumba transect; (e) Kisangani (river course from Landsat 8_9, source: https://earthexplorer.usgs.gov/)

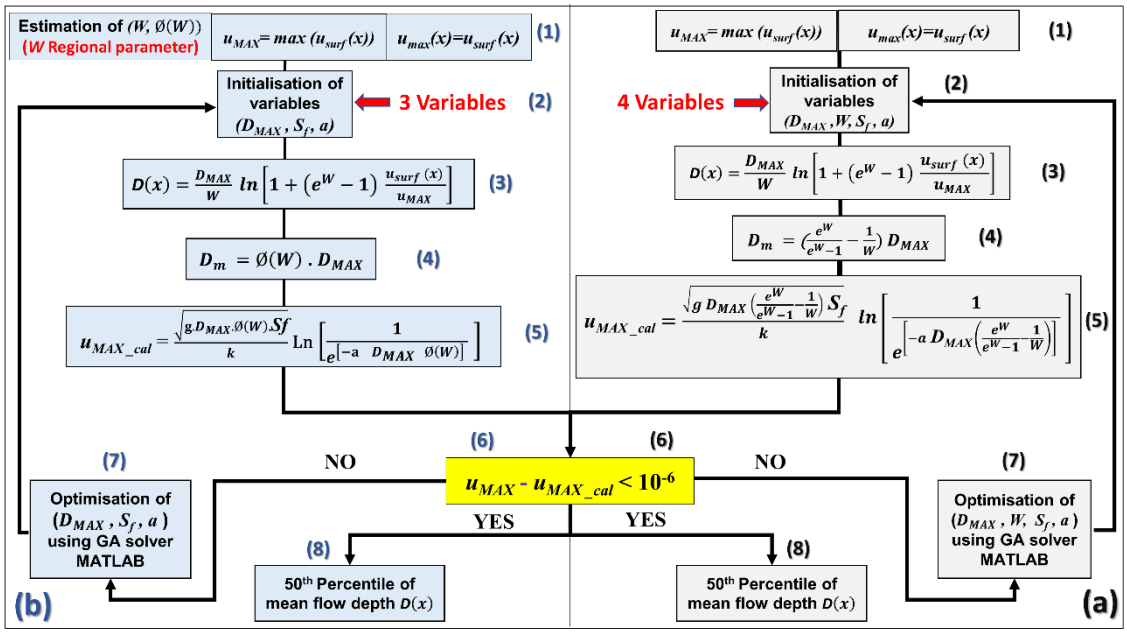

Figure 3. Process of the estimation of bathymetry using entropy theory: scenario (a) all the variables are optimised by GA solver, scenario (b): W is estimated based on measurements of (D_m, D_{MAX}) using ADCP.

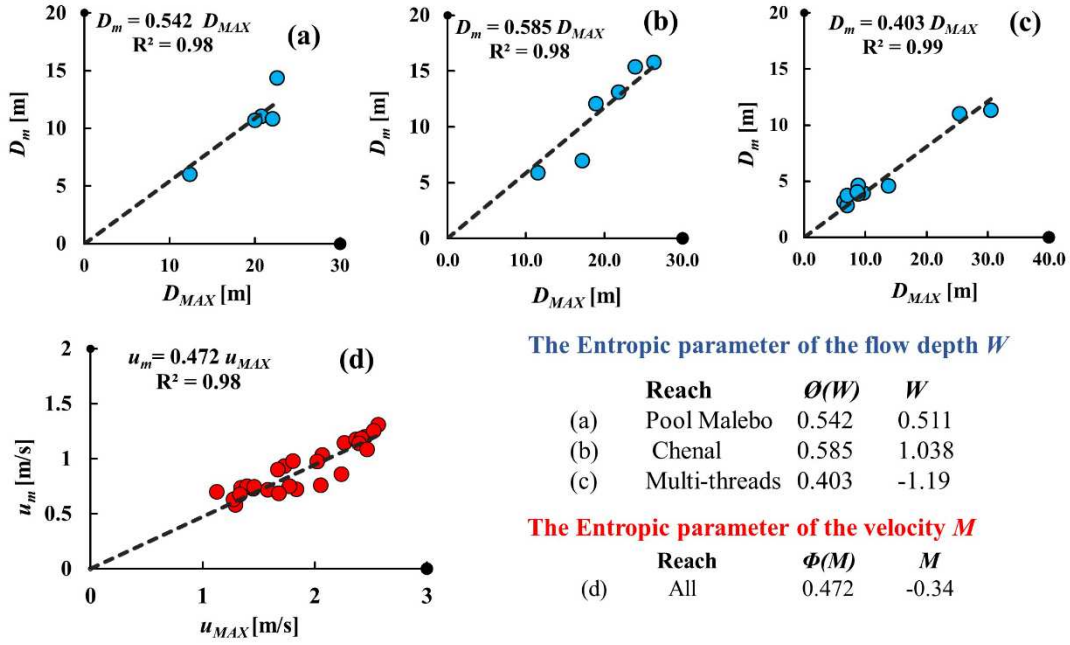

The Entropic parameter of the flow depth *W*

	Reach	*Ø(W)*	*W*
(a)	Pool Malebo	0.542	0.511
(b)	Chenal	0.585	1.038
(c)	Multi-threads	0.403	-1.19

The Entropic parameter of the velocity *M*

	Reach	*Φ(M)*	*M*
(d)	All	0.472	-0.34

Figure 4. Linear relationship between the mean and the maximum depth in the (a) Pool Malebo, (b) Chenal and (c) multi-thread reaches, (d) Linear Relationship between the mean and the maximum velocity in all the cross-section of the middle reach of the Congo River.

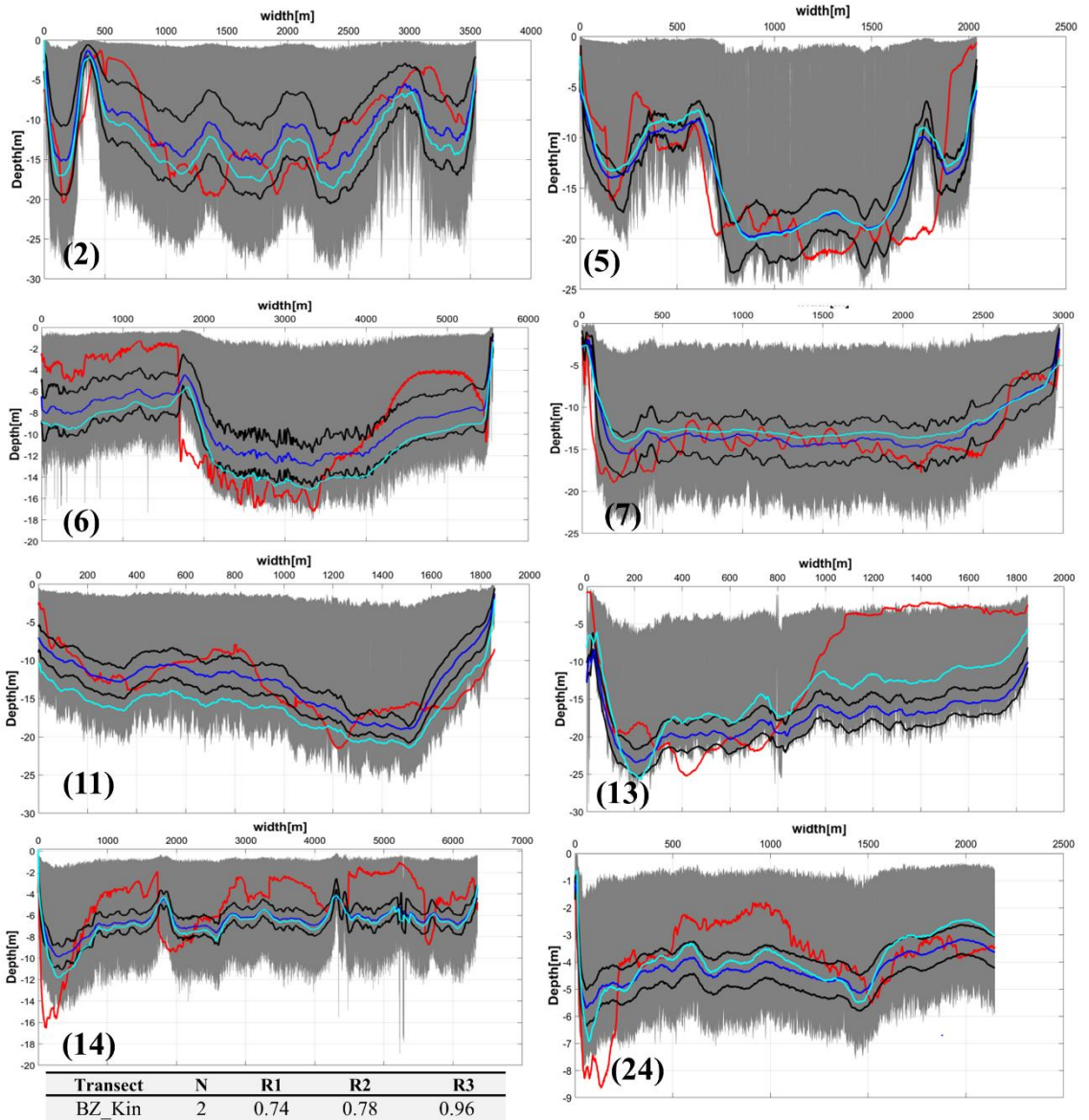

Transect	N	R1	R2	R3
BZ_Kin	2	0.74	0.78	0.96
Ndjili	5	0.53	0.57	0.99
Maluku	6	0.75	0.74	0.99
Maluku	7	0.70	0.71	0.99
Lenga	11	0.70	0.70	0.96
Lukolela	13	0.51	0.63	0.97
Clocke point	14	0.78	0.84	0.98
Lokutu	24	0.74	0.78	0.98

Figure 5. Comparison of *50th* estimated bathymetry using the entropy theory and measured profile using ADCP in the different transect of the middle reach of the Congo River, Correlation analysis is presented in (R1, R2, R3).

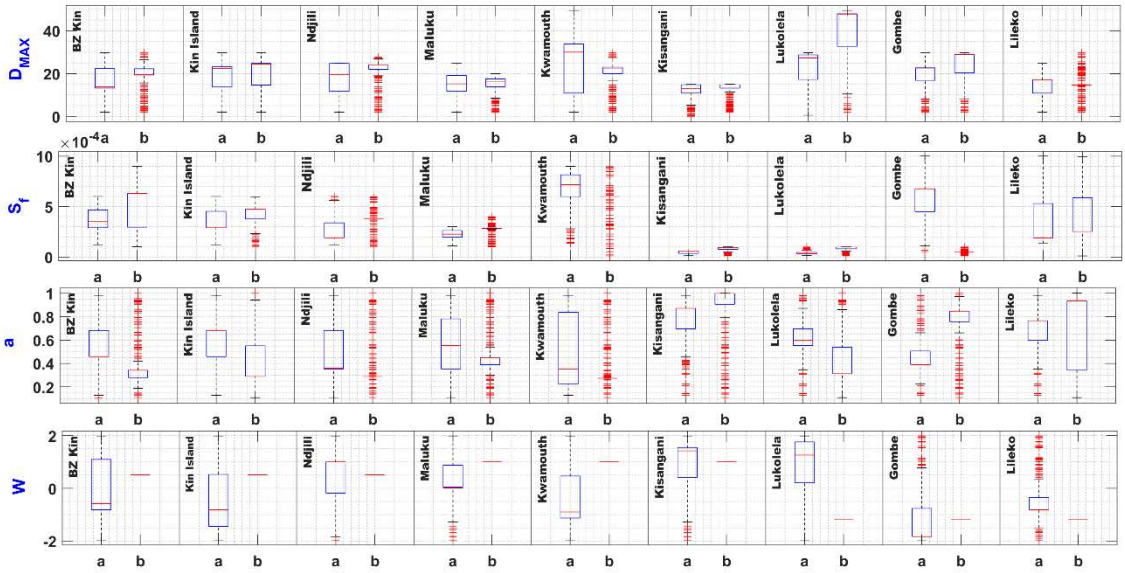

Figure 6. Boxplot of the range of variability of the different parameter (D_{MAX}, S_f, a, W) optimised by GA solver for 1000 realizations in both scenarios where scenario (a): W is estimated by GA solver, scenario (b) W is estimated based on measurements of (D_m, D_{MAX}).

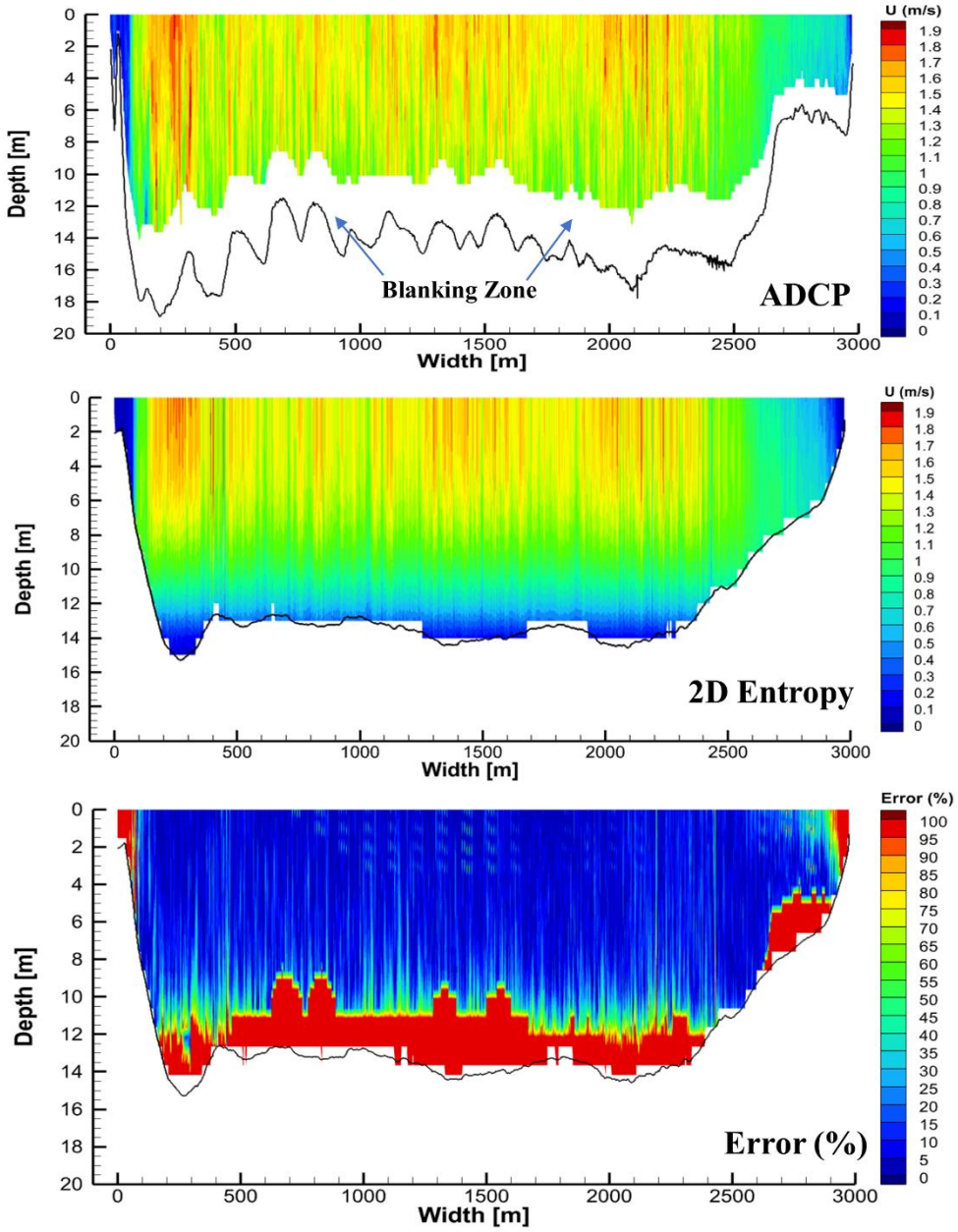

Figure 7. Velocity distribution in 2D using the entropy theory where the simulated bathymetry is used with error percentage dataset for the Maluku_2 transect compared to the observed via ADCP data.

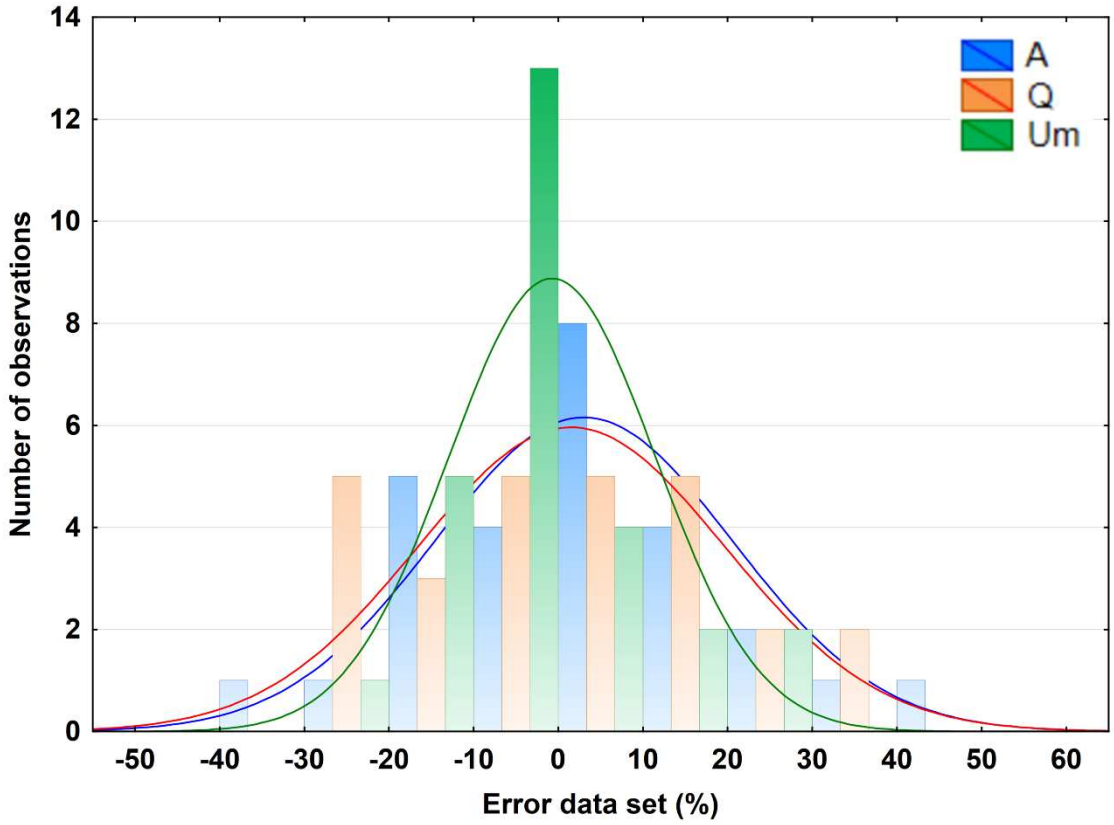

Figure 8. Histogram of the error data set for the different parameters with a normal fit distribution.

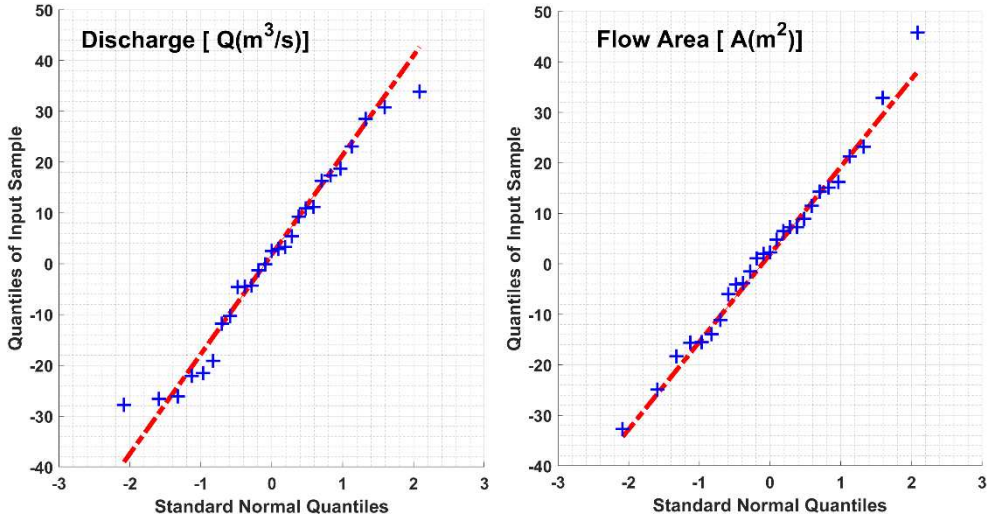

Figure 9. QQ Plot of sample data versus normal for the error between the estimated and observed results for both discharge and flow area.